Conductive filament structure in HfO_2 resistive switching memory devices

S. Privitera[1,*], G. Bersuker[2], S. Lombardo[1], C. Bongiorno[1], D. C. Gilmer[2]

1) Institute for Microelectronics and Microsystems (IMM), CNR, Zona Industriale, Ottava Strada 5, 95123 Catania, Italy

2) SEMATECH, 257 Fuller Road, 12203 Albany, New York, USA

We study the filament structure in 50 nm × 50 nm Resistive Random Access Memory (ReRAM) cells in the forming / set state with a Hf / HfO_2 / TiN metal-insulator-metal stack by scanning transmission electron microscopy in cross section view. We reveal the filament morphology and, by the measurement of filament size and electrical resistance, evaluate the average resistivity of the filament material. The combination of the various data indicates the nanostructure of the conductive filament.

I. INTRODUCTION

As the current non-volatile FLASH memory technology is approaching the scaling limits, several different memory concepts have been proposed and have attracted extensive attention, such as phase change memories, magneto-resistive random access memories (MRAM) and resistive switching memories (ReRAM). All these approaches are based on the possibility to change the resistance of a material by applying electric pulses and, in particular, ReRAM devices are considered to be very promising since they exhibit low power consumption, high switching speed, exceptional endurance and device fabrication simplicity, with potential for highest density arrays, as required for 3-D integrated circuit architecture [1,2,3]. A ReRAM device is based on a metal-insulator-metal (MIM) stack, in which a thin dielectric layer is sandwiched between two electrodes, and it is possible to form a conductive filament (CF) in the dielectric, connecting top and bottom metal electrodes. The filament formation may occur without involving the cation migration from an active electrode, but rather by local redox processes [4]. There are many materials showing this kind of resistive switching, such as TaO_2, HfO, NiO, CuO, TiO_2, and ZnO. In particular, Hf oxide is one the most promising materials, since it is already largely employed in CMOS technology.

The presence of a conductive filament inside a MIM largely modify its resistance. Formation of the filament is proposed to be caused by oxygen ion diffusion (induced by the applied electric field) out of a certain limited dielectric region and by subsequent field-temperature-driven migration of

*) Author to whom correspondence should be addressed. Electronic mail: stefania.privitera@imm.cnr.it

the released ions through the surrounding dielectric film [1,4,5]. Repeatable resistance switching is then described as involving as major limiting step the motion of these oxygen ions under an electric field bias back to the conductive filament, oxidizing a portion of the filament ('reset' to high resistance state, HRS), and their subsequent release and migration away from the filament ('set' to low resistance state, LRS) [4]. The physical dimensions of the filament and its physical structure throughout the hafnia dielectric is still subject of debate. Indeed, generally, the observation of a conductive filament (CF) in a real device is very difficult for several reasons. First, the CF is embedded between many surrounding layers, second, the filament size is expected to be only a few nanometers, third, the nucleation and growth of a conductive filament is a stochastic process, therefore the exact location of such a narrow filament is unpredictable. In the case of HfO_2, the observation is further complicated because Hf is a heavy element with a large number of electrons (atomic number Z=72). This means that by employing, as an example, a powerful technique such as Transmission Electron Microscopy (TEM), the electron beam is strongly diffused and back-reflected, obtaining poor images in transmission. These difficulties have prevented the observation of the CF in real devices based on HfO_2. Also, for all these reasons, previous *in-situ* TEM observations were done on specially-designed structures, different from those used in fabricated memory devices, and with different dielectric layers, typically characterized by lower atomic number Z, such as NiO, ZnO or SiO_2 [6,7,8]. However, the information on the physical mechanisms determining the filament formation, as well as its composition and size are crucial for a better understanding of the memory operation and for the device optimization and stability. Moreover, since the filament size is expected to be of the order of a few nanometers, the correlation between the size and the electrical properties, which could be strongly modified due to the confinement, can give more insight on the scaling properties of these memories.

In this work we have investigated a crossbar memory with size $50x50nm^2$ with HfO_2 dielectric and have employed the Scanning Transmission Electron Microscopy (STEM) to study the structure of the filaments in the low resistance state, after the forming process was completed. The measured filament size has been then correlated to the electrical resistance, obtaining insights on the filament resistivity, composition and nanostructure.

2. EXPERIMENTAL METHODS

The studied ReRAM cells are crossbar devices, 50 nm × 50 nm of size, with a TiN bottom electrode, a 5 nm HfO_2 dielectric, deposited by atomic layer deposition (ALD), and a metallic Hf top electrode with thickness 8 nm. On top of the metallic Hf, a thick TiN metal layer is deposited

and patterned. The memory is integrated with a transistor, which allows to limit the current during the device operation. Filament forming is achieved by applying forward biased (with the Hf top layer set as positive electrode) current-voltage (I-V) sweeps under well-defined current compliance conditions, in the 100 μA – 1 mA range. For the 1 mA current compliance case a HP4155 semiconductor parameter analyser was used, while for all the lower compliance levels the configuration with the transistor in series was employed.

To overcome the common problem in the TEM analyses of resistive switching devices, associated with difficulties to find the location of the filament within the entire volume of the memory cell, we have employed devices of a very small size, where the entire device volume is observable, allowing to collect data from the filament region. In such small area devices, to prepare cross-section specimens for TEM with the required accuracy, that is cross-sections of the entire device area of 50×50 nm^2, we have used a technique based on the Focused Ion Beam (FIB) sample thinning. The TEM and STEM analyses were performed in a JEOL 2010 electron microscope with a 200 kV accelerating voltage. In the STEM mode under the analysis condition, the minimum probe size was estimated to be about 0.5 nm. The microscope is also equipped with electron energy loss spectroscopy (EELS) imaging.

To study the morphology of the formed conductive filaments, both STEM in dark field configuration and EELS at low energy have been employed. The former is sensitive to the local average atomic number while the latter is strictly related to the plasmon losses, determined by the local chemical composition and phase. Resulting micrographs have a lateral resolution of about 1 nm. The information on the CF size, shape and composition has been extracted by fitting EELS spectra in the low energy region. The filament size measured by dark-field STEM imaging in any filament section has been determined as the local full-width at half-maximum (FWHM) of the number of counts. The error/resolution of both the dark field and EELS STEM measurements, and therefore the minimum observable filament size, is of the order of 1 nm.

3. RESULTS

Figure 1 (a) shows a TEM micrograph in bright field, acquired in a fresh device. The region of interest is very dark because of the thickness of the specimen and of the high electron beam diffusion and back-scattering. Figure 1 (b) shows the MIM device by STEM in dark field configuration, and at higher magnification. The image has been acquired using an annular detector, in order to enhance the mass contrast. The metallic Hf top electrode (brighter region) and the HfO_2 layer below are clearly distinguished, given the large difference in local charge density (Z-contrast).

On top of Hf a greyish region is also visible, corresponding to an additional Hf oxide layer present at the edges of the device.

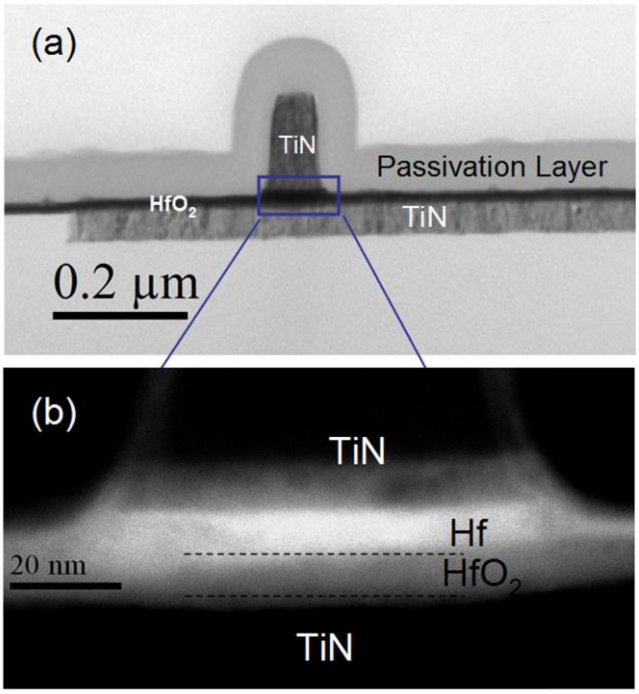

FIG. 1. (a) TEM bright field image of a crossbar device. (b) Details of the ReRAM device, acquired by STEM in dark field.

The pristine cell has a very high resistance, thermally activated with activation energy of about 0.1 eV [9]. The filament forming is achieved by applying I-V sweeps. Figure 2 (a) shows the I-V during forming, with a compliance of 500 µA. The filament is formed typically at +1.5 - +2.5 V and after forming the resistance is of the order of a few kΩ. In such a condition, the devices show a metallic behaviour, when conductance linearly decreases with temperature [4,9].

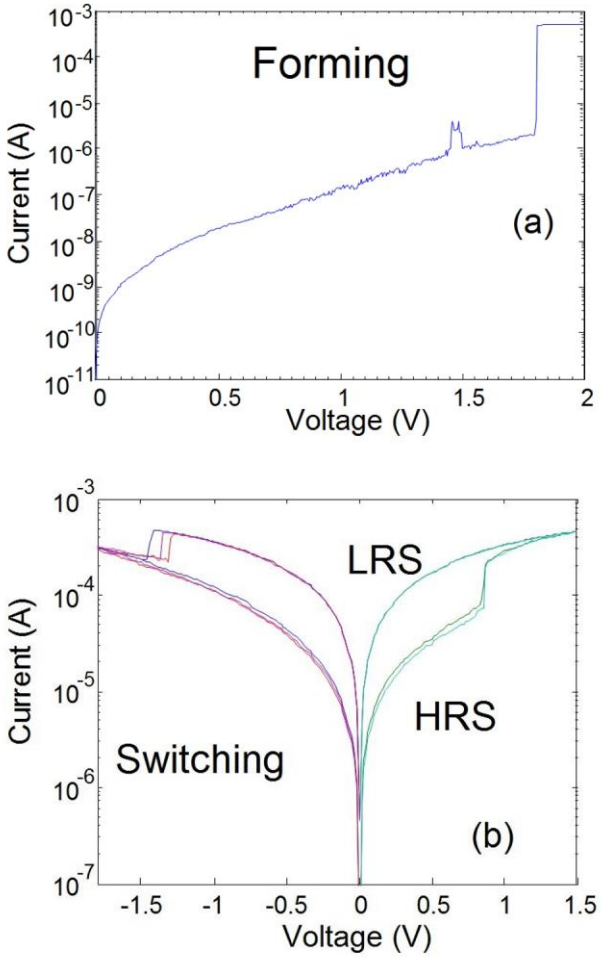

FIG 2. (a) Current-Voltage characteristic during filament forming. (b) Switching between the HRS and LRS.

Switching to a high resistance state is obtained by applying a negative bias, as shown in Fig. 2(b). In the HRS, the conductance is low and increases with temperature, as typical of semiconductors.

In the LRS the filament conductance can be written as $N \times G_Q$, where G_Q is the quantum conductance [10]

$$G_Q = \frac{2e^2}{h} \tag{1}$$

equal to about 1/13 $k\Omega^{-1}$, and the factor N is about 2-10 in the LRS.

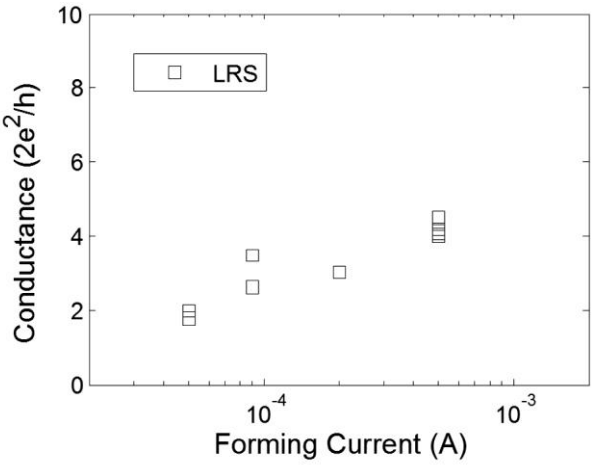

FIG. 3. Conductance in units of G_Q as a function of forming current compliance. Open symbols refer to the low resistance state (LRS).. Forming has been obtained using 1T1R configuration.

The conductance of the filament is strongly dependent on the forming current compliance, as shown in Fig. 3, where the conductance is plotted in units of G_Q. It is evident that, even in the LRS, the conductance is at the level of few G_Q units. This datum points to a physical size of the involved filament. In fact, according to Landauer [11], for a 1D metallic wire subjected to a small voltage drop V, the flowing current I is:

$$I/V = G = N \times G_Q \tag{2}$$

where N is the number of 1D sub-bands involved in the charge transport. For N = 1, only the first sub-band is involved and this suggests that the filament cross-section diameter, by assuming a simple cylindrical geometry and symmetry, is equal to $\lambda_F/2$, where λ_F is the conduction electron wavelength. Since in a metal λ_F is of the order of 1 nm [12], one should expect that the size of the metallic wire in the ReRAM cell is of that magnitude order, i.e, $\approx$ 1 nm. In similar stacks, the filaments described as Hf-rich in HfO_x-based ReRAM have been suggested to be ~1 to 3 nm depending on the compliance values during forming [4].

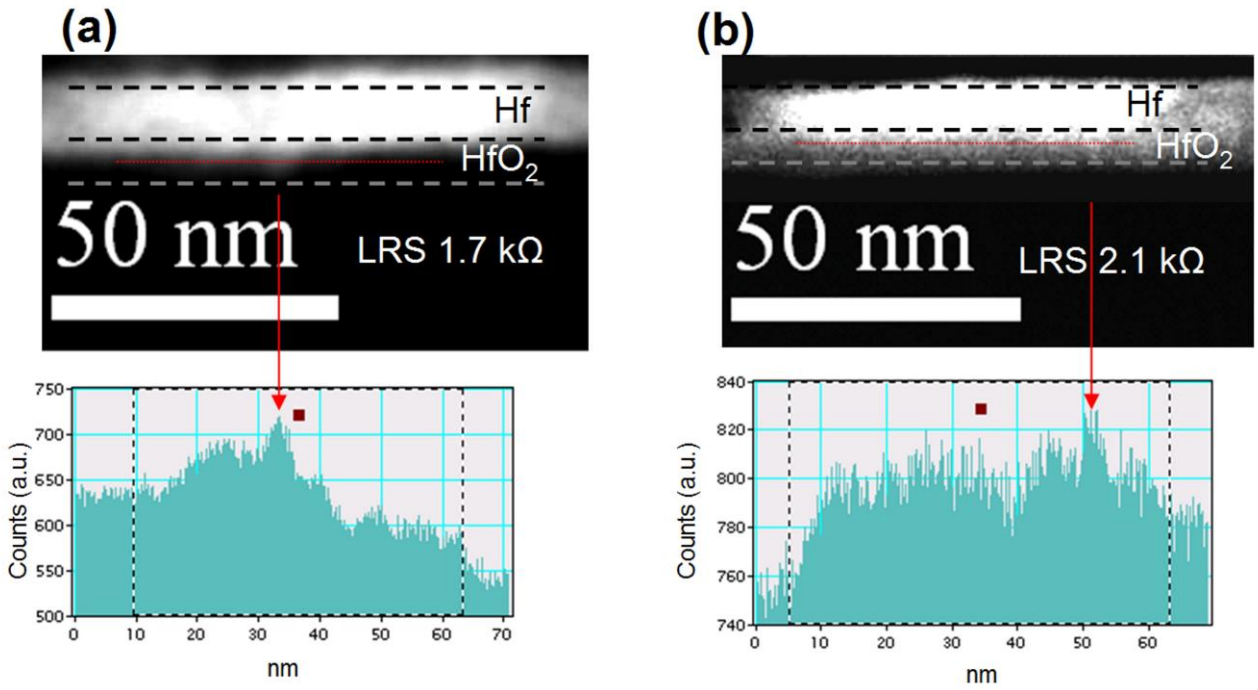

FIG. 4. Dark field STEM image of devices in the low resistance state, formed at 1 mA. (a) Resistance 1.7 kΩ, (b) resistance 2.1 kΩ. In the bottom, the corresponding intensity profile in the HfO_2 region, taken in the position indicated by the dotted line (red online). (a) is reprinted with permission from [9].

To measure the filament size we have therefore analysed by STEM some devices after the forming process. Fig. 4 (a) shows the Dark field STEM micrograph of a device after the filament forming, obtained by I-V sweep with 1 mA current compliance. The metallic Hf top electrode and the HfO_2 layer below are clearly distinguished. In addition, a brighter region in the HfO_2 layer is observed, approximately at the device center. This structure corresponds to the formed filament, with a measured resistance of about 1.7 kΩ in this case. The filament is of conical shape. From the local FWHM of the number of counts, on the side of the metallic Hf layer, the filament base is about 5.5 nm in diameter. Fig. 4 (b) shows another example of dark field STEM micrograph of a device after forming, again performed with the 1 mA current compliance. In this case the filament, again of a roughly conical shape, can be observed, but of a smaller size of about 3.5 nm at the base. In fact, as intuitively expected, a smaller size comparing to the case in Fig. 3 (a) corresponds to a higher filament resistance, of about 2.1 kΩ.

As alternative to the STEM imaging technique, we have also used a technique based on electron energy loss spectroscopy (EELS) at low energy. As shown in a previous work [9], EELS spectra taken in STEM mode, with the electron beam fixed in a certain position, strongly depend on the composition of the material under analysis..

The result of the fitting procedure discussed in [9], assuming the weighted superposition of the three spectra of the pure phases TiN, HfO_2, and metallic Hf is shown in Fig. 5 for the complete 50 ×

50 nm^2 MIM device (fresh device sample of Fig. 1). The colour charts refer, from top to bottom, to the metallic Hf, HfO_2, and TiN fitting coefficients, respectively. It is evident that the three layers are clearly detected with a relatively high spatial resolution. Note that the coefficients reported in Fig 5 and in Fig. 6 are normalized to the sum of the coefficients, in order to eliminate possible intensity variations due to thickness non-uniformities across the TEM specimen.

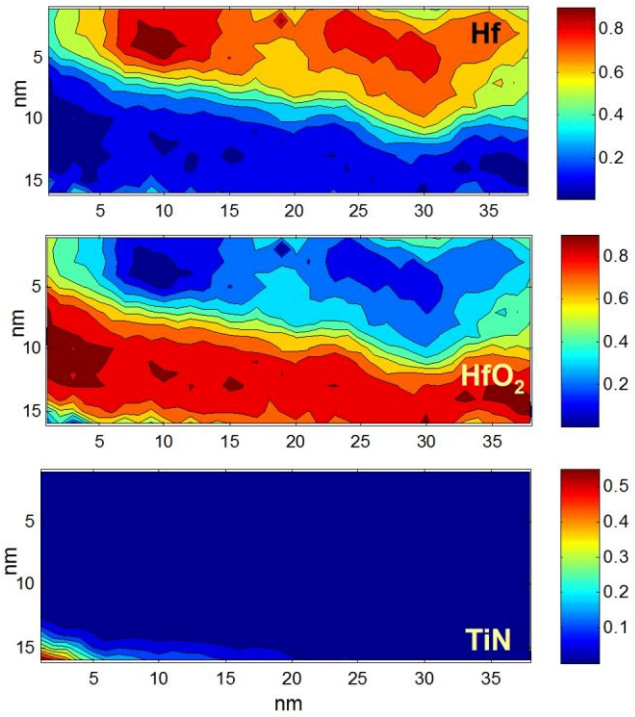

FIG. 5 Color charts of the metallic Hf, HfO_2, and TiN coefficients, obtained from fitting of the EELS spectra in each pixel. The sample is a fresh device, the same of Fig. 1.

The EELS STEM images of the devices of Fig. 4 (a) and (b), with the forming done using 1 mA current compliance condition are shown in Figs. 6(a) and 6(b), respectively. For the device shown in Fig. 4(a), a region of 5-6 nm width at the center of the HfO_2 layer is evident from the map (a "hole" in the HfO_2). Also a corresponding increase of the coefficient for metallic Hf is found. Thus, the filament appears to be a region of about 5 nm width, in which some of the HfO_2 is replaced by metallic Hf, consistent with the Z-contrast image of Fig. 4(a). The same is observed in Fig. 6(b), where the maps acquired in the device of Fig. 4(b) are shown. In this case, the filament has a width of about 2-3 nm, and it is located close to the right edge of the device.

As another example, Fig. 6(c) shows the EELS STEM image of a device subjected to a softer forming process, with a 0.5 mA current compliance. Also in this case, the maps show a decrease of the HfO_2 signal and a corresponding increase of the metallic Hf signal. In this sample, however,

two filaments, rather than one, are evidenced, and they exhibit rather small sizes, both being of the order of 2 nm or less.

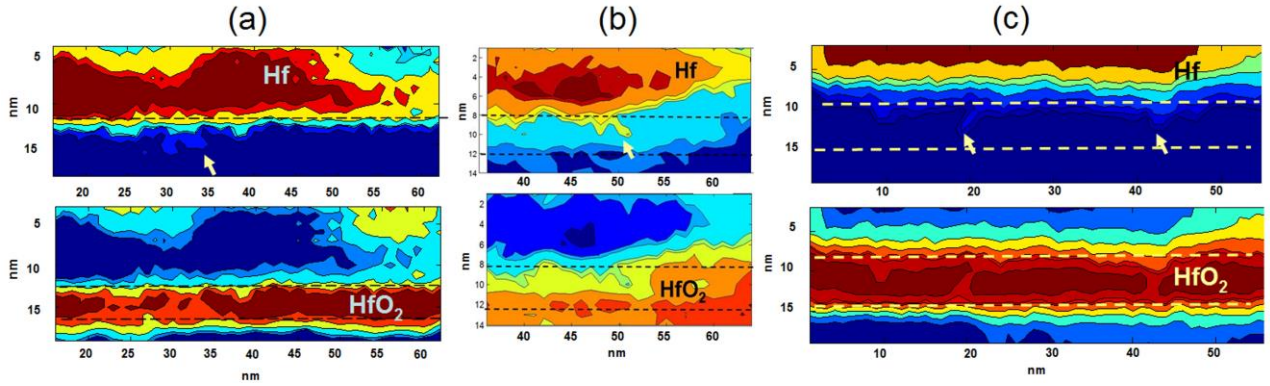

FIG. 6: Maps of the coefficients obtained from fitting to the EELS spectra at low loss for Hf (coefficient a1) and HfO_2 (a2). (a) and (b) show devices reported in Fig 4(a) and 4(b), respectively. (c) shows the coefficients obtained using a softer forming process (0.5 mA). The arrows indicate the filament positions. (a) is reprinted with permission from [9].

Overall, the STEM study and discussion above indicates that after the forming process the filament consists of a material with larger electron density than the surrounding environment of HfO_2, as demonstrated by the Z-contrast images, which show a brighter contrast in the filament. Moreover, the EELS images indicate that the filament region is a metallic-Hf rich material.

Additional information is gained by coupling the data on the filament size taken by the STEM images together with the measurement of the filament electrical resistance. In fact, the current linearly increases as a function of voltage and the resistance of the filament in the LRS can be measured by linear fit to data in the range 0 – 0.4 V. Considering the linearity of the current vs voltage, we have based our analysis on the assumption of a continuous filament and of resistance not dominated by tunnelling layers or influenced by current-limiting constrictions. This is reasonable in the case of LRS and we can therefore estimate its resistivity.

According to the second Ohm's law, in the metallic filament of cylindrical shape the resistance R is linked to the resistivity ρ:

$$R = \rho\, L\, /S \tag{3}$$

Where L and S are length and base area of the cylinder. In our case, a truncated cone is a better approximation to the filament shape, so:

$$R = \frac{\rho L}{\pi a b} \tag{4}$$

where a and b are the top and bottom base radii, respectively.

Fig. 7 shows the filament mean diameter $(2a+2b)/2$ data, measured by STEM imaging as a function of measured conductance (1/R). The continuous line is calculated according to (4), by assuming ρ =

0.25 mΩ×cm. The data fits well with (4), though the resistivity value of 0.25 mΩ×cm is significantly higher than that of bulk metallic Hf, of 0.034 mΩ×cm [13]. This difference can be due to a high degree of disorder, such as dangling bonds, oxygen related point defects, etc., or to a different composition, compared to pure metallic Hf.

To have more insight on the composition of the filament, we can compare the measured resistivity to that of Hf-oxide. The resistivity of stoichiometric HfO_2 (an insulator) is in the range of 10^{15} mΩ×cm, but it has been shown that in HfO_{2-x} films the resistivity drops steeply as the oxygen content decreases (below a threshold value) and it reaches a saturation value of about 0.4 mΩ×cm for large oxygen deficiency [14].

We have here estimated a lower resistivity value (0.25 mΩ×cm), suggesting that the filament should be fundamentally metallic in nature, but with a high degree of disorder. In such a condition, indeed, the carriers may suffer of many scattering processes and the mean free path is therefore expected to become very low. According to the Ioffe-Regel criterion [15] the usual theory of electrical conduction has to break down when the carriers mean free path λ approaches the interatomic distance a. Under these conditions ($\lambda \cong a$) we can calculate the maximum resistivity ρ_{max} beyond which the material becomes an insulator. According to both the Ioffe-Regel criterion [14] and Mott argumentations [16] $\rho_{max} = k\, a\, h/q^2$, where k is a factor equal to about 0.3 [14], or ~ 0.5 [15]. Considering the lattice parameter a = 0.32 nm of metallic Hf, the calculated value is ρ_{max} ~0.4 mΩ×cm. Such a value is higher, but close to the resistivity of 0.25 mΩ×cm that we have evaluated, indicating that the filament is a metal characterized by high level of disorder, since ρ approaching ρ_{max} means λ is very short, but not enough to prevent from the establishment of metallic transport. This observation is corroborated by the linear dependence of current versus voltage and by the increase of the resistance as a function of temperature observed in the LRS, as typical of metals. It is also reasonable to assume that the observed disorder may be produced by some Oxygen related defects. Indeed, a modeling of the nucleation of metallic rich clusters in HfO_2 [17] shows that slightly oxidized Hf (with composition close to $HfO_{0.2}$ and of critical radius around 0.4 nm), is the most stable phase of metallic character.

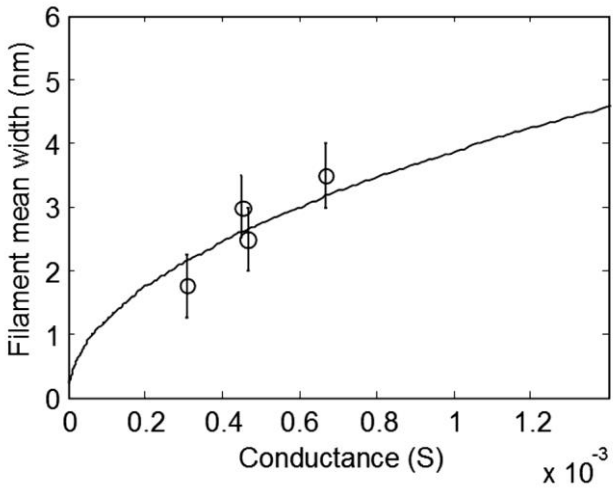

FIG. 7. Filament mean width (2*a*+2*b*)/2 measured by STEM as a function of Conductance, in units of (1/Ohm). Solid line is calculated according to (4), assuming ρ = 0.25 mΩ×cm.

Therefore, on the base of our observations, the forming current compliance seems to essentially control the filament size, rather than its composition, at least in the range of currents down to 500 µA, giving rise to the formation of metallic conductive filaments with different diameter but with almost the same resistivity. It is therefore reasonable to assume that the filament size is proportional to the energy dissipated during the forming process. At compliance values of 500 µA the filament size is close to the limit resolution of the present technique, therefore we are not able to see filaments formed at lower current. To evaluate the size and the composition of smaller filaments a STEM equipment with higher resolution and smaller devices should be employed.

4. CONCLUSIONS

The conductive filament in HfO_2-based ReRAM has been observed using the analytical techniques of STEM and EELS. Use of very small devices and careful sample preparation employing sample thinning by FIB allowed for capturing the entire device structure in the STEM/EELS field of view. Having the entire structure in the field of STEM/EELS analysis led to the ability to locate and analyse very small conductive filaments. The observed conductive filaments in the HfO_2-based ReRAM devices have a conical shape with mean diameters of ~1-3 nm. Based on the measured conductance of the low resistance state, filament diameters, and its calculated resistivity the filament is primarily comprised of a disordered metallic Hf, possibly partially oxidised.

REFERENCES

[1] Waser R, Dittmann R, Staikov G, Szot K. Redox-Based Resistive Switching Memories – Nanoionic Mechanisms, Prospects, and Challenges. Adv. Mater. 2009*;* 21:2632-2633. 10.1002/adma.200900375

[2] Bersuker G, Gilmer DC, In Nishi Y, Editor. Advances in Non-volatile Memory and Storage Technology, 1st Edition. Cambridge: Woodhead Publishing; 2014, p. 288.

[3] Akinaga H, Shima H. Resistive Random Access Memory (ReRAM) Based on Metal Oxides. Proc. Of the IEEE 2010; 98:2237-2251

[4] Bersuker G, Gilmer DC, Veksler D, Kirsch P, Vandelli L, Padovani A, Larcher L, McKenna K, Shluger A, Iglesias V, Porti M, Nafría M. Metal oxide resistive memory switching mechanism based on conductive filament properties. Journal of Appl. Phys. 2011; 110:124518

[5] Guan X, Yu S, Wong HSP. On the switching parameter variation of metal-oxide RRAM—part I: Physical modelling and simulation methodology. IEEE Trans. Electron Dev. 2012, 59:1172-82

[6] Liu Q, Sun J, Lv H, Long S, Yin K, Wan N, Li Y, Sun L, Liu M. Real-Time Observation on Dynamic Growth/Dissolution of Conductive Filaments in Oxide-Electrolyte-Based ReRAM. Adv. Mater. 2012, 24:1844-1849

[7] Yao J, Zhong L, Natelson D, Tour JM, In situ imaging of the conducting filament in a silicon oxide resistive switch. Nature Scientific Rep. 2012, 2:242.

[8] Calka P, Martinez E, Delaye V, Lafond D, Audoit G, Mariolle D, Chevalier N, Grampeix H, Cagli C, Jousseaume V, Guedj C, Chemical and structural properties of conducting nanofilaments in TiN/HfO_2-based resistive switching structures. Nanotechnology 2013, 24**:**085706

[9] Privitera S, Bersuker G, Butcher B, Kalantarian A, Lombardo S, Bongiorno C, Geer R, Gilmer DC, Kirsch PD. Microscopy study of the conductive filament in HfO_2 resistive switching memory devices. Microelectronics Engineering 2013,109:75-78

[10] Long S, Lian X, Cagli C, Cartoixà X, Rurali R, Miranda E, Jimènez D, Perniola L, Liu M, Sune J, Quantum-size effects in hafnium-oxide resistive switching. Appl. Phys. Lett. 2013, 102:183505

[11] Ferry DK, Goodnick SM, Transport in Nanostructures, Cambridge: Cambridge University Press; 1997, p. 124.

[12] C. Kittel, Introduction to Solid State Physics, Eight Edition, Wiley, New York, 2005, ISBN 047141526X, p. 139

[13] Desai PD, Chu PK, James HM, Ho CY, Electrical resistivity of selected elements. J. Phys. Chem. Ref. Data 1984, 13:1069

[14] Hildebrandt E, Kurian J, Müller MM, Schroeder T, Kleebe HJ, Alff L, Controlled oxygen vacancy induced p-type conductivity in HfO_{2-x} thin films Appl. Phys. Lett. 2011, 99**:**112902

[15] Ioffe AF, Regel AR, in Gibson AF, Editor. Progress in Semiconductors Vol. 4. Heywood; 1960, p. 237–291.

[16] Mott N. Electrons in glass. Nobel Lecture 1977

[17] McKenna KP, Optimal stoichiometry for nucleation and growth of conductive filaments in HfO_x Modelling Simul. Mater. Sci. Eng. 2014, 22:025001